RSC Advances

ROYAL SOCIETY OF CHEMISTRY

www.rsc.org/advances

Synthesis of Ag/PANI@MnO_2 Core–Shell Nanowires and Their Capacitance Behavior

Chao Pan[1,2], Yinhua Lv[1],Huimin Gong[1], Qike Jiang[1], Shu Miao[1], Jingyue Liu[1,3*]

[1]Energy Research Resources Division, Dalian Institute of Chemical Physics, Dalian 116023, China

[2] College of Science, Dalian Ocean University, Dalian 116023, China

[3]Department of Physics, Arizona State University, Tempe, Arizona 85287, United states

* Corresponding author. Tel.: +8641184379707.

E-mail address: jingyueliu@msn.com.

Keywords: MnO_2, composite, core-shell architecture, supercapacitor

Abstract. Polyaniline (PANI) nanowires coated with Ag nanoparticles and MnO_2 nanoflakes were fabricated via a facile two-step *in situ* oxidative polymerization process, and their applications for electrochemical energy storage were explored. Morphological study confirmed the formation of Ag nanoparticles on the PANI surface that was uniformly coated by MnO_2. Electrochemical tests showed that the ternary Ag/PANI@MnO_2 nanoscale architectures displayed a high specific capacitance of 518.0 F g^{-1}at the current density of 0.1 A g^{-1}, with a retention ratio of 88.4% after 1,600 cycles at the current density of 1.0 A g^{-1}. The good performance is attributed to the synergistic effects of the different components of the Ag/PANI@MnO_2nanocomposite system.

Introduction

Supercapacitors have attracted intense interests because of their higher power density (compared to batteries) and higher energy density (compared to conventional dielectric capacitors).[1-3] In recent years, the ever-increasing demands for energy storage applications have attracted significant research efforts in developing novel electrode materials with higher storage capacity, better rate capability and cycling stability.[4, 5]Transition-metal oxides, due to their

pseudo-capacitance behavior render much higher energy density than those based on carbon materials and conducting polymers. [6, 7]Among the transition metal oxides, MnO_2 is the most competitive candidate for supercapacitors due to its low cost, natural abundance, environmental safety, a very high theoretical specific capacitance (SC) of 1370 Fg^{-1} [8], and wide operating potential range in mild electrolyte.[9, 10]However, its intrinsically poor electronic conductivity limits the practical capacitance to only about one-sixth to one-fifth of the theoretical value. To further increase the electrical conductivity, composites of conducting polymers and MnO_2 have been investigated.[11, 12]The conductive polymers act not only as 3-dimensional (3-D) scaffolds but also provide better conductive channels, resulting in enhanced specific capacitance and cycle stability. PANI has been recognized as one of the most promising pseudo-capacitive materials (supporting Information Figure S1) suitable for the next generation of supercapacitors since it has the merits of high pseudo-capacitance, light weight, low cost, controllable electrical conductivity, high energy density, environmental friendliness, and facile synthesis[13-1516-19] Moreover, it exhibits excellent SC in the range typically between 500 to 3400 F/g depending on preparation conditions,[20] which is substantially larger than that of conventional carbon-based electrodes (~100-200 F/g).[21]Among various desirable morphologies, one-dimensional (1D) nanostructured materials as building components in electrochemical energy storage are more attractive because they provide short diffusion path lengths to ions, leading to high charge/discharge rates.[22] Most of the present strategies involve the formation of a 1D conducting polymer−MnO_2 composite in confined nanochannels through electrochemical or chemical reduction of KMnO4.[23]Jiang *et al*[24] reported the synthesis of MnO_2–PANI core–shell nanofibers by simply soaking polyaniline nanofibers in a $KMnO_4$ solution. Han *et al.*[23] reported that the combination of MnO_2 nanorods and conducting

polymer nanofibers into 1D hierarchical structure had excellent electrochemical properties.

To further improve the SC of MnO_2-PANI nanocomposites, extensive research work has been focused on ternary composite films as electrodes. In these uniquely structured systems, each component contributes a specific functionality to achieve the goal of enhancing capacitance and energy density. Ternary composites have demonstrated high specific capacitances, good rate capability, and good cycling stability.[25] It has been reported that Ag/MnO_2nanocomposite system exhibited higher SC than pure MnO_2.[26-29]It was proposed that the addition of Ag nanoparticles could reduce the electrical resistance of oxide pseudo-capacitor materials. Furthermore, the incorporation of Ag into PANI is thought to increase the system's electrical conductivity and thus electrochemical storage capacity. For example, Xie*et al.*[30] synthesized PANI−Ag nanocable arrays and obtained a specific capacitance as high as 850 F/g at 10 mV/s sweep rate. A PANI-Ag system with a Ag loading of 0.9 wt% exhibited almost a 2-fold higher SC than pure PANI.[31] Therefore, rational design of a low cost and facile ternary nanoarchitecture system with better electrochemical performance, although challenging, is desirable. We selected to develop the Ag/PANI@MnO_2 core–shell ternary nanocomposite to achieve this goal.

In the present work, we fabricated new ternary Ag/PANI@MnO_2 core–shell nanowires. The Ag/PANI@MnO_2 system exhibited high specific capacitance and retention rate. At an applied current densityof0.1 Ag^{-1}, the maximum specific capacitance of Ag/PANI@MnO_2reached 518.0 F g^{-1}, which is about 4-, 2-, and 2-fold higher than the capacitance of using PANI, Ag/PANI, and PANI@MnO_2, respectively.

Experimental section

Chemical reagents

All chemicals used in these experiments were of analytical grade and were purchased from Sinopharm Chemical Reagent Co. Ltd. (China).The aniline was distilled under reduced pressure before use and all the other chemicals were used as received. The deionized water were prepared by a Milli-Q Plus system (Millipore, France) with a measured electrical resistivity of 18.2 MΩ.

Synthesis of PANI nanowires

The aniline monomer was distilled under reduced pressure and H_2SO_4 and ammonium persulfate ($(NH_4)_2S_2O_8$, APS) were used as the dopant and oxidant, respectively. A typical synthesis procedure for PANI nanowires was as follows: 0.2 mol sulfuric acid and 0.03mol aniline were added to a 0.2 L aqueous solution, under stirring in ice bath for about 30 min. Then, another 0.2 L aqueous solution containing APS was added dropwise to the mixture and stirred for 10 min. The molar ratio of ANi:APS was 4:1. The polymerization was carried out at 0°Cfor 6 h. The obtained powders were filtered and washed several times with distilled water to remove residual APS oxidant, and then were dried at 80 °C for 12 h.

Synthesis of Ag/PANI nanowires

The Ag/PANI were prepared according to a previously described method.[32, 33] In a typical procedure, 1M $AgNO_3$ solution was made with deionized (DI) water and stirred for 10min using a magnetic stirrer at room temperature. Then 0.05 g PANI nanowires were added to the above solution followed by 5 min ultrasonic mixing. The mixture was then subjected for 1 h stirring. Ag/PANI nanowires were obtained by drying the mixture in an oven at 80 °C for 12 h.

The incorporation of Ag nanoparticles was carried out by redox reaction between PANI and Ag^+ ions in solutions. The emeraldine form of PANI is oxidized with silver nitrate to pernigraniline while the Ag^+ ions are reduced to metallic silver.[34]

Synthesis of Ag/PANI nanowires@MnO_2 nanocomposite

In a typical procedure, 0.05 g of as-synthesized Ag/PANI nanowires were added into 20 mL 0.015 M $KMnO_4$ aqueous solution under stirring. After the addition of $KMnO_4$ to aqueous solution containing conducting polymer nanowires, the redox reactions between conducting polymers and $KMnO_4$should occur near the surfaces of the conducting polymer nanowires. The MnO_2clusters nucleated and grew on the conducting polymer nanowires.[23] The mixed solution was sealed in a 30 mL Teflon-lined stainless steel autoclave, and heated in an oven at 120 °C for 2 h, and then cooled down to room temperature in air. The Ag/PANI nanowires@MnO_2 powders were filtered, washed with DI water, and dried at 80 °C for 12 h. The content of MnO_2 is 32.4% by inductively coupled plasma atomic emission spectroscopy (ICP, 7300DV,Perkinelmer) analysis.

Synthesis of PANI@MnO_2 nanowires

MnO_2@PANI composites were synthesized by following the same procedure as synthesis of Ag/PANI nanowires@MnO_2, except that 0.05 g of the as-synthesized PANI nanowires, instead of the Ag/PANI nanowires, were used.

Characterization

The morphology and crystal structure of the products were examined by afield-emission scanning electron microscope (FESEM; JEOL, JSM-7800F) equipped with an energy dispersive X-ray (EDX) system (Oxford Instruments X-Max), transmission electron microscope (TEM; JEOL, JEM-2100, 200 kV), and X-ray photoelectron spectroscopy (XPS, Escalab 250, Al Ka).XRD measurements were performed on a D8 X-ray diffractometer (X'pert Pro-1), employing monochromatized Cu K_α incident radiation.

The electrochemical properties of the as-synthesized Ag/PANI nanowires@MnO_2

nanocomposites were investigated using a three-electrode cell configuration at room temperature. The working electrodes were fabricated by mixing the prepared powders with 10 wt% acetylene black and 5 wt% polyvinylidenefluoride (PVDF) binder. A small amount of N-methylpyrrolidinone (NMP) was added to the mixture to produce a homogeneous paste. The mixture was pressed onto nickel foam current-collectors (1.0 cm^2) to make electrodes (The Ni foam has good stability in Na_2SO_4 electrolyte, as shown in ESI Fig. S2). The coated active material electrodes were dried at 80 □ overnight in a vacuum oven. The loading density of the active material is 4.0 mg/cm^2. Before the electrochemical test, the as-prepared electrode was soaked in 1M Na_2SO_4 solution overnight.

Electrochemical tests of cyclic voltammetry (CV) and galvanostatic charge–discharge (GCD) were performed on a CHI660D electrochemical workstation (Shanghai Chenhua Instruments Co., China). All measurements were carried out in a three-electrode cell with a working electrode, a platinum plate counter electrode and an Ag/AgCl reference electrode (SCE). The electrolyte was 1 M Na_2SO_4 aqueous solution (Polyaniline energy storage mechanism is the use of its oxidation-reduction reaction, namely conversion of aniline and its quinone structure to achieve. The main role of the outside of the electrolyte is to provide freedom of movement of the positive and negative ions, thus sulfate electrolyte can be available.) . The potential was swept between 0 and 0.9 V at a scanning rate of 5-100 mV/s. EIS tests were carried out with a frequency loop from 10^5 Hz to 0.01 Hz using perturbation amplitude of 5 mV. The SC of the electrode is calculated from the GCD curves based on the following equation:

$$C_m = \frac{I\Delta t}{m\Delta V} \quad (1)$$

Where C_m($F\ g^{-1}$) , I (A), m(g), Δt(s) and ΔV(V) are the SC of the electrodes, the discharge

current, the mass of the active materials, the discharging time and the discharging potential range, respectively.

Results and discussion

Characterization of Ag/PANI nanowires@MnO_2nanocomposite

The XRD patterns of PANI nanowires, Ag/PANI, PANI@MnO_2, and Ag/PANI nanowires@MnO_2 nanocomposite are shown in Figure 1. For the Ag/PANI, the sharp crystalline peaks at 2θ values of 38.09°, 44.30°, 64.38°, and 77.33° correspond to the face-centered cubic (fcc) phase of Ag (111), (200), (220), and (311), respectively.[35, 36]The same crystalline peaks were observed for the Ag/PANI nanowires@MnO_2 composite. The existence of sharp peaks in both Ag/PANI and Ag/PANI nanowires@MnO_2 clearly indicates the presence of large Ag nanoparticles with a crystalline nature in the composite. For MnO_2, two peaks at 36.38° and 65.35° were observed, and can be indexed to the monoclinic K-birnessite MnO_2 (JCPDS no. 80-1098). For pure PANI, two peaks at 20.39° and 25.25° were observed, representing the periodicity parallel and perpendicular to the polymer chain of PANI.[37] It was observed that all of the XRD patterns show a broad peak at a 2θ value of 15−27°. This is mainly because of the amorphous nature of PANI.

Surface measurements by XPS are carried out for PANI nanowires, Ag/PANI and Ag/PANI nanowires@MnO_2. XPS N 1s spectra of PANI and Ag/PANI samples are presented in Figure2(a and b).Usually, the N peak in XPS spectra of PANI can be deconvoluted into three distinct curves, related to the quinoid imine, the benzenoid amine and the positively charged nitrogen. Fig. 2a and 2b show the two major peaks related to quinoid imine and benzenoid amine, which are observed at 399.33 eV and 400.43eV for PANI nanowires, whereas they are observed at 398.55 eV and

399.68eV for Ag/PANI. There is a small variation observed for binding energies between PANI nanowires and Ag/PANI due to the presence of Ag in PANI. The Ag (3d) spectrum of the Ag/PANI sample is shown in Figure 2(c). The Ag ($3d_{5/2}$), and Ag ($3d_{3/2}$) peaks are located at the binding energies of 368.55 (0.72) and 374.52eV (0.01), respectively. The Mn 2p spectrum is analyzed in Fig.2d. Both the Mn $2p_{3/2}$ peak at 642.05 eV and the Mn $2p_{1/2}$ peak at 653.71 eV are clearly observed, in good agreement with the energy splitting of the standard spectrum of MnO_2.[38] The peak-to-peak separation between Mn $2p_{1/2}$ and Mn $2p_{3/2}$ level is about 11.7 eV, suggesting the 4^+ oxidation state for Mn,in agreement with those reported in literature.[39] Figure2e shows the deconvoluted O 1s spectrum, where asharp peak located at 529.69 eV and two broad peaks located at 531.20 and 532.68 eV can be observed. This spectrum is in good agreement with literature reports of 529.3–530.3 eV for oxide, 530.5–531.5 eV for hydroxide, and 531.8–532.8 eV for water.[40]

Figure3a shows the pure PANI nanowires with a diameter of 60–80 nm and a length around 500 nm. Figure 3c and 3d represent the secondary electron (SE) and backscattered electron (BSE) images of the as-synthesized Ag/PANI composites, respectively. The BSE image clearly shows that the PANI nanowires were covered by small Ag nanoparticles. The Ag tends to bind with the nitrogen sites of PANI leading to interchain linkage between many adjacent PANI chains by coordination.[41] The electron density on the nitrogen atoms of PANI decreases upon the formation of Ag complex, making the nitrogen atoms electron deficient. Such a configuration is supposed to enhance the conductivity of the composite system. Hence the increase in the conductivity of the PANI electrodes by Ag coating may help to enhance the specific capacitance.[36] After the loading of MnO_2, a layer of uniform nanoscale floccules on the Ag/PANI nanowires (vermicular structures)

is observed in the ternary composite material (Fig. 3(e, f)), suggesting a core-shell nanostructure.EDS analysis of the ternary Ag/PANI@MnO_2 composite sample confirms the existence of Ag and Mn.

Figure 4a shows the TEM image of PNAI nanowires coated with porous MnO_2. It can be seen that the MnO_2 nanoflakes directly grow on the PNAI nanowires. TEM images of Ag/PANI (Fig. 4b) show the attachment of Ag nanoparticles on the PANI surfaces. The Ag nanoparticles are uniformly distributed with a spherical shape and an average diameter of 2−5 nm. The agglomerated Ag nanoparticles (indicated by yellow circles) are also observed to have a diameter of 10−30 nm. Figure 4c and 4d show the TEM images of Ag/PANI nanowires coated with porous MnO_2. It can be seen that the porous MnO_2 layer is composed of numerous tiny nanoflakes, these MnO_2nanoflakes are interconnected and uniformly distributed on the Ag/PANI nanowires.

Evaluation of capacitive performance

Figure5a shows the CV (cyclic voltammograms) curves of PANI, Ag/PANI, PANI@MnO_2, and Ag/PANI@MnO_2 samples tested in 1 M Na_2SO_4 at potential intervals from 0 V to 0.9 V vs. Ag/AgCl reference electrode at a scan rate of 5 mV/s. The CV curves clearly deviate from a rectangle, the typical shape for electric double-layer capacitors, indicating that redox processes occurred. All the samples were reversibly reduced and oxidized in the Na_2SO_4 electrolyte, which suggests that pseudo-capacitive processes occurred. For the CV curve of PANI, two pairs of redox peaks at 0.32, 0.52 V and 0.40, 0.79 V appear. These are due to the redox transition of PANI between the semiconducting state (leucoemeraldine form) and the conducting state (polaronicemeraldine form). For Ag/PANI and Ag/MnO_2/PANI composites, an additional anodic peak was observed at 0.20 V, and 0.18 V, respectively, due to the oxidation of Ag. The slight shift

of this anodic peak is caused by electrode resistance. For PANI@MnO_2, the sample exhibits rectangular and symmetric CV curves, proving their ideal pseudo-capacitive nature with a fast charge–discharge process.[42]. Among all of the electrode materials, Ag/MnO_2/PANI nanocomposite showed the highest specific capacitance value of 440 F/g at the 5 mV/s scan rate, whereas PANI, PANI@MnO_2 and Ag/PANI exhibited specific capacitance of 96.8, 228.2 and169.8F/g, respectively. The enhanced electrochemical performance of the ternary Ag/PANI@MnO_2 composite electrode can be understood as a combined effect of several factors. First, the uniform coating of MnO_2 on the PANI nanowires with Ag nanoparticles yields a superior nanoarchitecture for fast diffusion of ions which may enhance the specific capacitance. Second, the Ag nanoparticles in the nanocomposite greatly increase the electrical conductivity,[43] there is good interaction between PANI and MnO_2 for the enhancement of the specific capacitance. And third, the protective MnO_2 layers prevent structural damage to the PANI during charging and discharging processes. Compared to the CV of PANI electrodes, considering the PANI and Ag contribute small capacitance to the electrode. So the major capacitance contributor is MnO_2 (Supporting Information Figure S3, Table S1), the MnO_2 layer enables fast and reversible redox reactions to improve the specific capacitance, thus contribute to a high overall specific capacitance.[24, 44] the CV curves of Ag/ PANI@ MnO_2 in 1 M Na_2SO_4 at different scan rates are shown in Fig.5b. For all samples, the SCs decrease with increasing scan rates, revealing a charge storage process due to diffusion electrochemistry. Electrolytes (i.e., Na^+ and H^+) can only reach the outer surface of the electrodes at high scan rates. At low scan rates, the electrolytes have enough time to get into deep pores leading to high SC.

For all samples, the SCs of all as-prepared electrodes were also determined by galvanostatic

charge–discharge (GCD) measurements. The GCD curves of PANI, PANI@MnO_2, Ag/PANI, Ag/PANI@MnO_2 at 0.1 A/g current density are compared in Fig. 6.The curvature of the GCD curves indicates the pseudo-capacitive behavior of the electrodes. The IR drops in Fig.6a (0.22, 0.17, 0.04 and 0.02 V for PANI, Ag/PANI, PANI@MnO_2 and Ag/PANI@MnO_2, respectively) indicate that the thin layer of Ag nanoparticles and MnO_2 can greatly reduce the internal resistance, and thus facilitates the transport and collection of electrons. The Ag/PANI@MnO_2 nanocomposite has the longest discharge time, which indicates that this electrode has the best electrochemical performance. The SC of the electrode can be calculated according to equation (1). The specific capacitance of Ag/PANI@MnO_2 (518.0 F/g) is much higher than those of PANI@MnO_2 (273.1 F/g), Ag/PANI (218.3 F/g) and PANI (119.7 F/g) at the same current density of 0.1 A/g. Figure 6b depicts the galvanostatic charge/discharge plot of Ag/PANI@MnO_2 composite at different current densities of 0.1, 0.2, 0.3, 0.5 and 1 A/g. The charge curves are symmetrical to their discharge counterparts. Same trend is observed for Ag/PANI@MnO_2 when further increasing current density (Figure 6c), indicating the robustness of the as-prepared hybrid Ag/PANI@MnO_2 as electrode materials. Figure 6d shows the specific capacitance of Ag/PANI@MnO_2 as a function of cycling number at a current density of 1.0 A g^{-1} in the voltage range 0 ~ 0.9 V. The SC shows a slight increase for the first 200 cycles before decreases monotonically, probably due to the insufficient contact of composites with Na_2SO_4 aqueous solution at the beginning of electrochemical measurement.[45, 46] A retention of 88.4% of the highest capacitance was obtained after 1600 continuous galvanostatic charge/discharge cycles. The higher cyclic stability of the Ag/PANI@MnO_2 composite can be attributed to the presence of MnO_2 over Ag nanoparticles coated PANI surfaces.

The electrochemical properties of Ag/PANI@ MnO_2 were further evaluated with electrochemical impedance spectroscopy (EIS). The impedance spectra of composite electrodes were measured in the frequency range of 100 kHz to 0.01 Hz (Fig. 7). The equivalent series resistance (ESR) of pristine PANI, Ag/PANI and Ag/PANI@MnO_2 obtained from the intersection of the Nyquist plot at the x-axis is 1.22, 1.17, and 1.05 V, respectively. Considering the similar morphology of Ag/PANI and Ag/PANI@MnO_2, the difference in ESR of electrodes can be attributed to the different conductivities of electrode materials. The smaller ESR of Ag/PANI@MnO_2 than Ag/PANI suggests the decreased charge transfer resistance in the presence of MnO_2 nanoflakes. The high resistance of ion transfer in Ag/PANI would be attributed to high charge density, resulting in low capacitance.

Conclusions

In conclusion, we have prepared a high-performance electrode material by decorating PANI nanowires with MnO_2coated on Ag nanoparticles, via a facile two-step *in situ* oxidative polymerization process. The as-prepared ternary composite exhibits a high specific capacitance of 518.0 F g^{-1} with good rate and cycling stabilities in 1 M Na_2SO_4 aqueous solution. The presence of Ag nanoparticles on PANI nanowires provides a least resistance path to electrons. The synergistic effects of the combined pseudo-capacitive contributions from both the PANI and MnO_2 enhance the overall capacitance. The synthetic approach, discussed in this paper, to nanoarchitectured systems with desired properties is general and can be extended a many other similar systems for developing supercapcitors and batteries with enhanced performances.

Acknowledgements

We acknowledge the financial support of the National Natural Science Foundation (NO. 21102033), the China Postdoctoral Science Foundation (2014M551138). JL acknowledges the funding of the College of Liberal Arts and Sciences of Arizona State University.

Notes and references

1. A.Burke, *J. Power Sources*, 2000, **91**, 37-50.
2. M. Winter and R. J. Brodd, *Chem. Rev.* , 2004, **104**, 4245-4270.
3. J. R.Miller and P.Simon, *Science*, 2008, **321**, 651-652.
4. C.Liu, F. Li, L. Ma and H. Cheng, *Adv.Mater.* , 2010, **22**, E28-E62.
5. P. Simon and Y.Gogotsi, *Nat. Mater.*, 2008, **7**, 845-854.
6. J. Jiang, Y. Y. Li, J. P. Liu, X. T. Huang, C. Z. Yuan and X. W. D. Lou, *Adv. Mater.*, 2012, **24**, 5166-5180.
7. T. F.Otero and I. Cantero, *J. Power Sources*, 1999, **81-82**, 838-841.
8. G.Zhang, L. Yu, H. E. Hoster and X. W. Lou, *Nanoscale*, 2013, **5**, 877-881.
9. F. Wang, S. Y. Xiao, Y. Y. Hou, C. L. Hu, L. L. Liu and Y. P. Wu, *RSC Adv.*, 2013, **3**, 13059-13084
10. X.Zhang, X.Sun, H.Zhang, D.Zhang and Y. Ma, *Electrochim. Acta*, 2013, **87**, 637-644.
11. R. K.Sharma, A. Karakoti, S. Seal and L. Zhai, *J. Power Sources*, 2010, **195**, 1256-1262.
12. S. R.Sivakkumar, J. M.Ko, D. Y.Kim, B. C.Kim and G. G. Wallace, *Electrochim. Acta*, 2007, **52**, 7377-7385.
13. G.Wang, X.Lu, Y.Ling, T.Zhai, H.Wang, Y.Tong and Y.Li, *ACS Nano*, 2012, **11**, 10296-10302.
14. G.Yu, X.Xie, L.Pan, Z.Bao and Y.Cui, *Nano Energy* 2013, **2**, 213-234.
15. X.Peng, K.Huo, J.Fu, X.Zhang, B.Gao and K.Chu, *Chem. Commun.* , 2013, **49**, 10172.
16. G.Wang, L.Zhang and J. Zhang, *Chem. Soc. Rev.*, 2012, **41**, 797-828.
17. G.Yu, L.Hu, N.Liu, H.Wang, M.Vosgueritchian, Y.Yang, Y.Cui and Z. Bao, *Nano Lett.*, 2011, **11** 4438-4442.
18. G. A.Snook, P.Kao and A. S. Best, *J . Power Sources*, 2011, **196** 1-12.
19. L.Chen, L.J.Sun, F. Luan, Y. Liang, Y.Li and X. X. Liu, *J. Power Sources*, 2010, **195** 3742-3747.
20. Q.Zhang, E.Uchaker, S. L.Candelaria and G. Cao, *Chem. Soc.Rev.*, 2013, **42**, 3127-3171.
21. X.Lu, M.Yu, T.Zhai, G.Wang, S.Xie, T.Liu, C.Liang, Y.Tong and Y. Li, *Nano Lett.*, 2013, **13**, 2628-2633.
22. A. L. M. Reddy, M. M. Shaijumon, S. R. Gowda and P. M. Ajayan, *Nano Lett.*, 2009, **9**, 1002-1006.
23. J. Han, L. Y. Li, P. Fang and R. Guo, *J. Phys. Chem. C*, 2012, **116**, 15900-15907.
24. H. Jiang, J. Ma and C. Z. Li, *J. Mater. Chem.*, 2012, **22**, 16939-16942.
25. J. Kim, H. J. Akbar, Inamdar, Y. Jo, J. Han, H. Kim and H. Im, *Energy* 2014, **70**, 473-477.
26. Y. H. Wang and I. Zhitomirsky, *Mater. Lett.*, 2011, **65**, 1759-1761.
27. M. Sawangphruk, S. Pinitsoontorn and J. Limtrakul, *J. solid. state. electro*, 2012, **16**, 2623-2629
28. G. N. Zhang, L. Zheng, M. Zhang, S. H. Guo, Z. H. Liu, Z. P. Yang and Z. L. Wang, *Energy Fuel*, 2012, **26**, 618–623.
29. L. B. Ma, X. P. Shen, Z. Y. Ji, G. X. Zhu and H. Zhou, *Chem. Eng. J.*, 2014, **252**, 95–103.

30. Y.Xie, Z. Song, S. Yao, H. Wang, W.Zhang, Y. Yao, B. Ye, C. Song, J. Chen and Y. Wang, *Mater. Lett*, 2012, **86**, 77-79.
31. D. S. Patil, J. S. Shaikh, S. A. Pawar, R. S. Devan, Y. R. Ma, A. V. Moholkar, J. H. Kim, R. S. Kalubarme, C. J. Park and P. S. Patil, *Phys. Chem. Chem. Phys.*, 2012, **14**, 11886–11895.
32. J. Han, J. Dai, C. Q. Zhou and R. Guo, *Polym Chem*, 2013, **4**, 313-321.
33. J. Han, L. Y. Li and R. Guo, *Macromolecules*, 2010, **43**, 10636–10644.
34. J. Stejskal, J. Prokeš and I. Sapurina, *Mater Lett* 2009, **63**, 709-711.
35. M. M.Ayad, N.Prastomo, A.Matsuda and J. Stejskal, *Synth. Met.* , 2010, **160**, 42-46.
36. S. Dhibar and C. K. Das, *Ind. Eng. Chem. Res*, 2014, **53**, 3495-3508.
37. Q. Jia, S.Shan, L.Jiang and Y. Wang, *J. Appl. Polym. Sci.* , 2009, **115**, 26-31.
38. Z. Liu, R. Ma, Y. Ebina, K. Takada and T. Sasaki, *Chem. Mater.* , 2007, **19**, 6504-6512.
39. C.Zhu, S. Guo, F. Y., L. Han and S. Wang, *Nano Res*, 2011, **4**, 648-657.
40. D. Yan, P. X. Yan, S. Cheng, J. T. Chen, R. F. Zhuo, J. J. Feng and G. A. Zhang, *Cryst. Growth Des.*, 2009, **9**, 218-222.
41. J.Li, M. Cui, Y. Lai, Z.Zhang, H. Lu, J. Fangand and Y. Liu, *Synth. Met.*, 2010, **160**, 1228-1233.
42. H. Jiang, L. P. Yang, C. Z. Li, C. Y. Yan, P. S. Lee and J. Ma, *Energy Environ. Sci.*, 2011, **4**, 1813-1819.
43. M. M. Oliveira, E. G. Castro, C. D. Canestraro, D. Zanchet, D. l. Ugarte, L. S. Roman and A. J. G. Zarbin, *J. Phys. Chem. B*, 2006, **110**, 17063-17069.
44. J. Kim, H. Ju, A. I. Inamdar, Y.Jo, J. Han, H.Kim and H.Im, *Energy Environ. Sci.*, 2014, **70**, 473-477.
45. Y. Liu, H. Wang, J. Zhou, L. Y. Bian, E. W. Zhu, J. F. Hai, J. Tang and W. Tang, *Electrochim. Acta*, 2013, **112**, 44-52.
46. G. Q. Han, Y. Liu, L. L. Zhang, E. J. Kan, S. P. Zhang, J. Tang and W. H. Tang, *Science Report* 2014, **4**, 1-7.

Figure captions

Figure 1. XRD patterns of (a) PANI, (b) Ag/PANI, (c) PANI@MnO_2, and (d) Ag/PANI nanowires@MnO_2 composite.

Figure 2. N1s XPS core level spectra of (a) PANI, (b) Ag/PANI; (c) Ag (3d) XPS spectrum of Ag/PANI; (d) XPS spectrum of Mn 2p of Ag/PANI nanowires@MnO_2; (e) XPS spectrum of O1s of Ag/PANI nanowires@MnO_2.

Figure 3. FE-SEM image of (a) PANI nanowires; (b) PANI@MnO_2 nanowires; (c) Ag/PANI nanowires; (e)Ag/PANI@MnO_2 composite; BSE image of (d) Ag/PANI nanowires and (f) Ag/PANI@MnO_2 composite, (g) EDS spectrum of Ag/PANI @MnO_2 composite.

Figure 4. (a) TEM image of PANI@MnO_2, (b) TEM images of Ag/PANI composites. (c, d) TEM images of Ag/PANI@ MnO_2composites.

Figure 5. (a) Cyclic voltammograms of the samples recorded at a scan rate of 5 mV/s for PANI, Ag/PANI, PANI@MnO_2, and Ag/PANI@MnO_2 composite. (b) Cyclic voltammograms at different scan rates of Ag/PANI@MnO_2.

Figure 6. GCD curves of (a) specific capacitance of PANI, PANI@MnO_2, Ag/PANI and Ag/PANI@MnO_2 at 0.1 A/g current density; (b) Ag/PANI@MnO_2 at different current density; (c)specific capacitance curves of PANI, PANI@MnO_2, Ag/PANI and Ag/PANI@MnO_2 composites at different current densities; (d) specific capacitance as a function of cycle number at 1.0 A g^{-1} of the Ag/PANI@MnO_2.

Figure 7. Nyquist impedance plots of PANI, Ag/PANI and Ag/PANI@MnO_2 composites

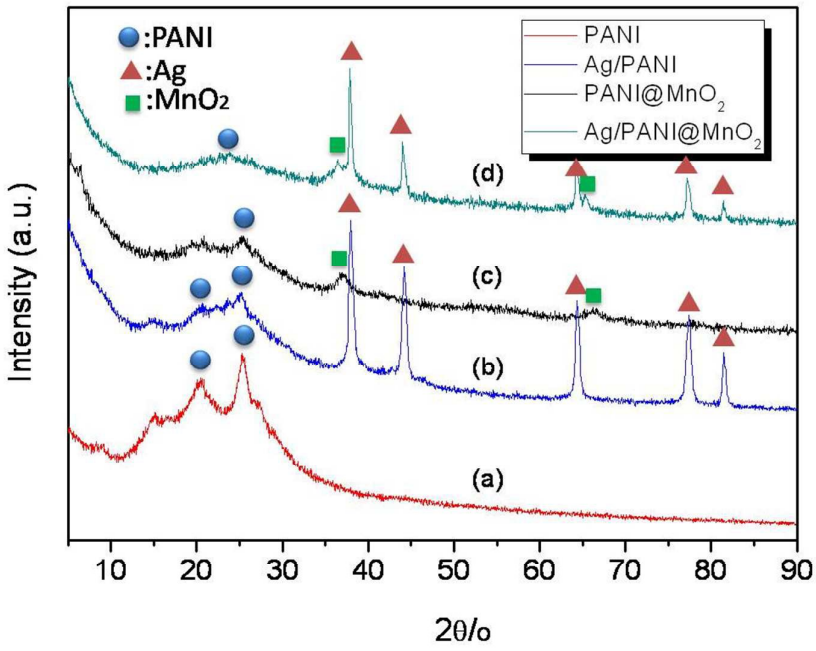

Figure 1

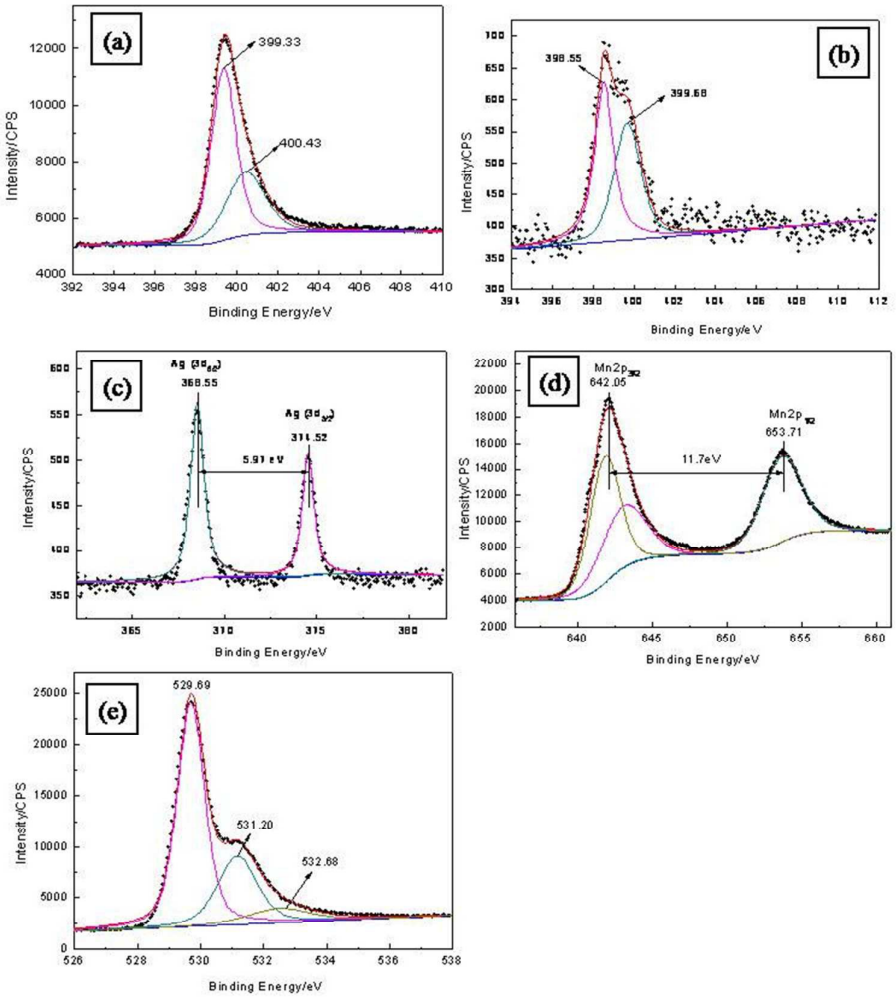

Figure 2

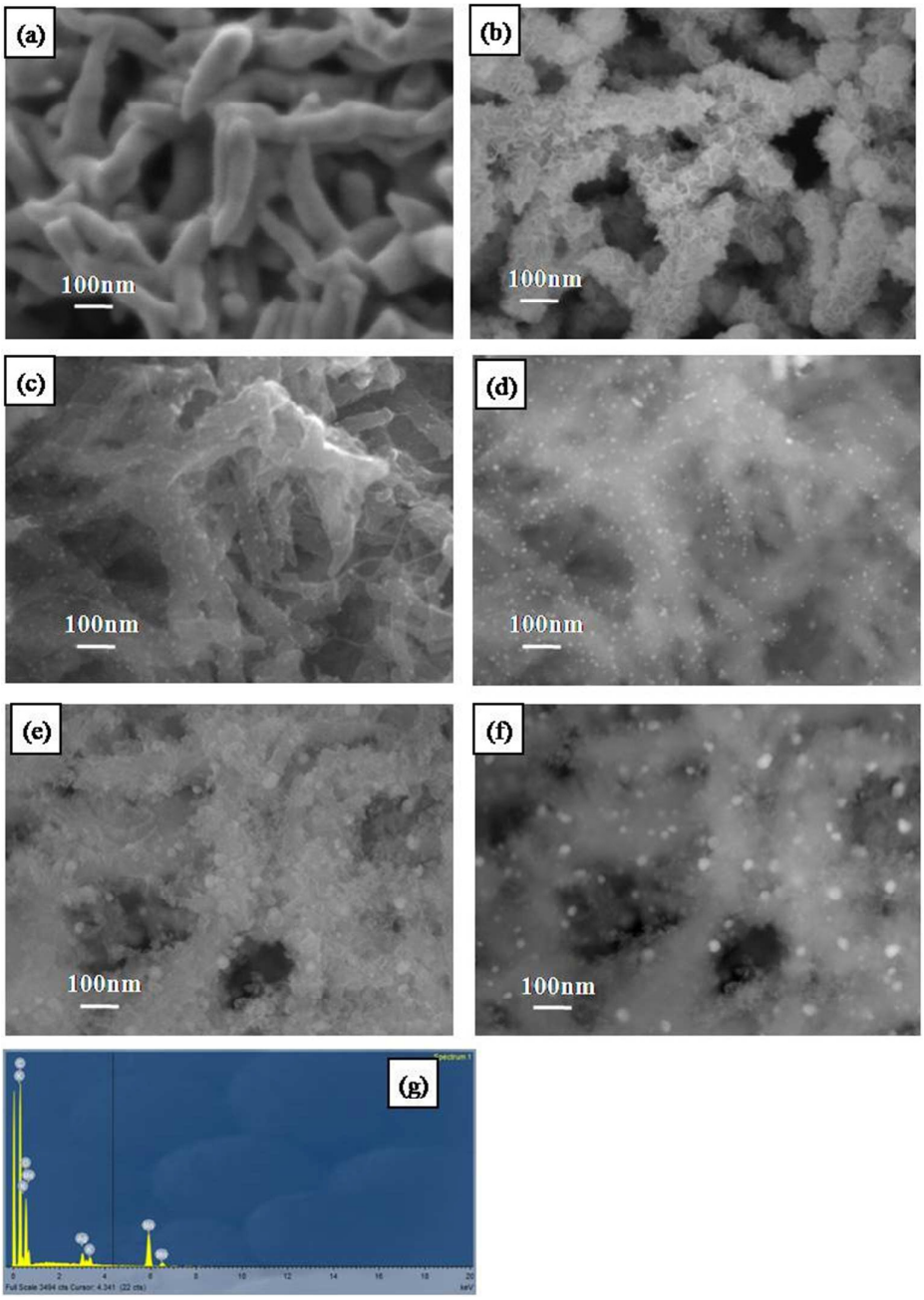

Figure 3

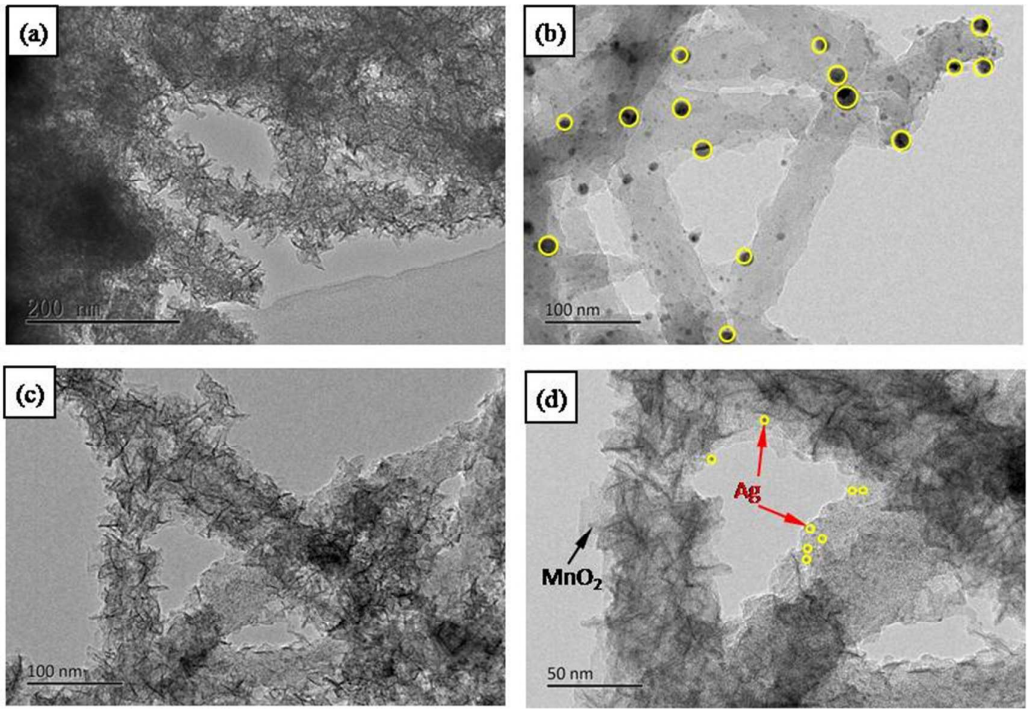

Figure 4

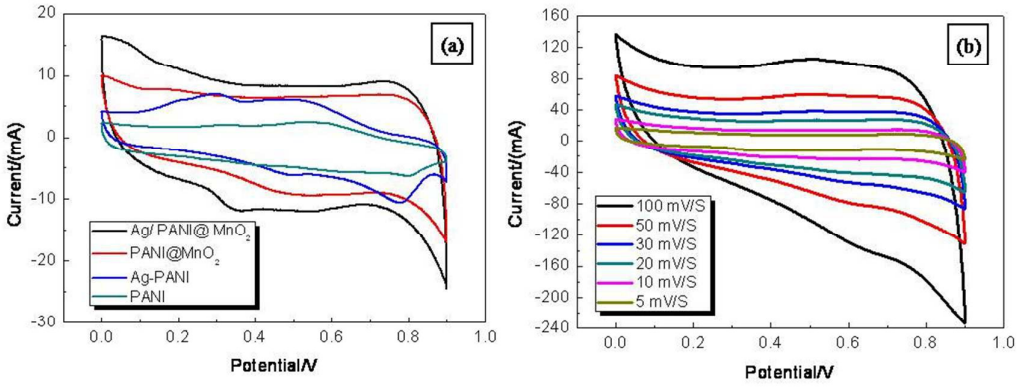

Figure 5

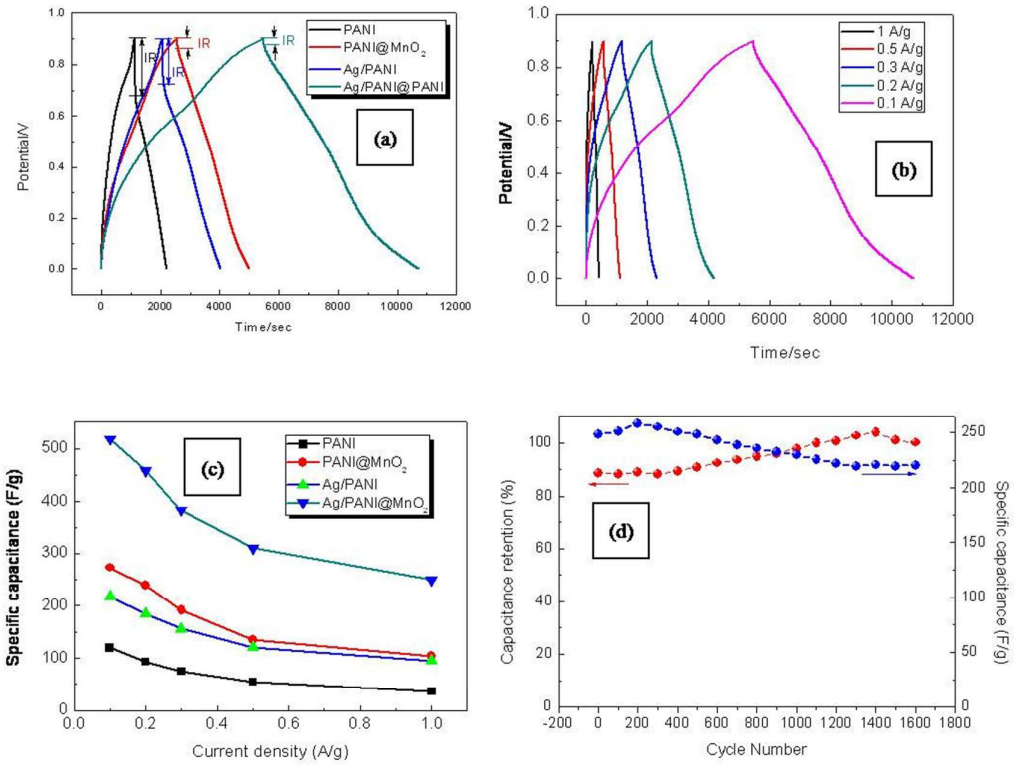

Figure 6

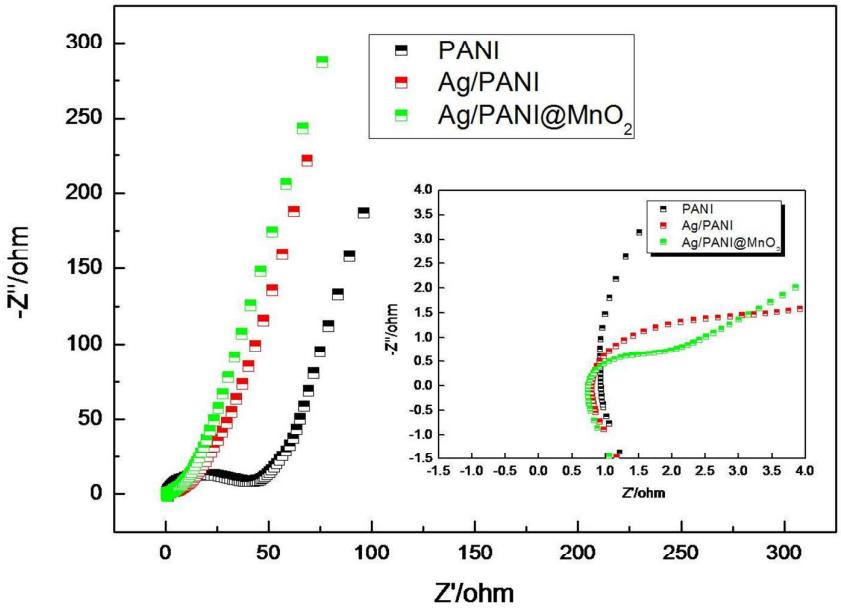

Figure 7

Graphical abstract

A novel ternary hybrid material of 1D Ag/PANI@MnO_2 core–shell nanowires are synthesized by a quick and facile two-step process. The Ag/PANI@MnO_2 composites electrode exhibited a high specific capacitance of 518.0 F g^{-1}at the current density of 0.1 A g^{-1}, with a retention ratio of 88.4% after 1600 cycles at the current density of 1.0 A g^{-1}. The good performance of PANI/GECF is attributed to the synergistic effects of the Ag/PANI@MnO_2 nanocomposite and core-shell nanowires architecture.